Effect of Pressure on the Structure and Electrical Conductivity of Cardanol–Furfural–Polyaniline Blends

Fernando G. Souza, Jr,[1] Marcos T. D. Orlando,[2] Ricardo C. Michel,[1] José Carlos Pinto,[3] Tainá Cosme,[3] Geiza E. Oliveira[4]

[1]*Instituto de Macromoléculas, Universidade Federal do Rio de Janeiro, Centro de Tecnologia, Bloco J, Ilha do Fundão, Rio de Janeiro, 21941-914RJ, Brazil*
[2]*Departamento de Física/Centro de Ciências Exatas, Universidade Federal do Espírito Santo, Avenida Fernando Ferrari, s/n, Goiabeiras, Vitória, 29075-910, Brazil*
[3]*Programa de Engenharia Química/Instituto Alberto Luiz Coimbra de Pós-Graduação e Pesquisa em Engenharia, Universidade Federal do Rio de Janeiro, Cidade Universitária, CP 68502, Rio de Janeiro, 21945-970RJ, Brazil*
[4]*Departamento de Química/Centro de Ciências Exatas, Universidade Federal do Espírito Santo Av. Fernando Ferrari, s/n, Goiabeiras, Vitória, 29075-910, Brazil*

Received 24 April 2009; accepted 23 May 2010
DOI 10.1002/app.32848
Published online 9 September 2010 in Wiley Online Library (wileyonlinelibrary.com).

ABSTRACT: Pressure-sensitive polymers that simultaneously present reasonable electrical conducting properties, useful thermosetting behavior, and softness are hard to develop. To combine these properties into a single material, a cardanol-based phenolic resin was prepared and blended *in situ* with polyaniline (PAni). The final polymer blend was composed of a soft solid material that could not be dissolved in ordinary solvents. Samples were characterized through X-ray scattering, Fourier transform infrared (FTIR) spectroscopy, and electrical conductivity and pressure sensitivity measurements. FTIR results indicate that the insertion of PAni into the blends did not change the chemical nature of the resin. According to wide-angle X-ray scattering results, PAni was dispersed homogeneously in the final polymer samples; this improved the sensitivity of the electrical conductivity to pressure variations, as confirmed through electromechanical tests. Pressure sensitivity and electromechanical analyses indicated that the produced blends could be used as pressure-sensing materials. Among the tested materials, the blends containing 5 wt % PAni·H_2SO_4 presented the largest compression sensitivity values. Finally, it was shown for the first time through XRD analyses under pressure that PAni chains were considerably disturbed by compressive stresses. © 2010 Wiley Periodicals, Inc. J Appl Polym Sci 119: 2666–2673, 2011

Key words: biopolymers; nanocomposites; resins; sensors; WAXS

INTRODUCTION

Nowadays, there a general agreement about the importance of promoting the sustainable use of planetary resources[1] to preserve the environment for future generations. As a result of the probable lack of petroleum in the near future[2] and of the inevitable increase in oil costs, the production of polymer materials based on alternative raw materials must be tirelessly encouraged.[1–6] Unfortunately, the production of polymer materials from renewable resources usually leads to high costs and low yields.[1,7] Therefore, the search for renewable materials that can be polymerized at high conversions must also be encouraged.[1,8]

One of the most promising renewable resources to be used for the production of polymer resins is cashew nut shell liquid (CNSL). CNSL is a cheap byproduct of the cashew industry and is a naturally occurring substituted phenol that can take part in a large number of distinct chemical reactions. For this reason, it can be used for the manufacture of a multitude of useful products and can replace phenol in many applications with equivalent or even improved performance.[1,7] The main component of CNSL is cardanol, which is an acid phenol derivative[1,2,8] that presents a metasubstituent composed of a C15 unsaturated hydrocarbon chain containing one to three double bonds.[1,2]

Cardanol is an acidic species[1,2,9] (see Fig. 1), which can be used to promote the secondary doping of polyaniline (PAni), which is doped primarily with dodecyl benzene sulfonic acid or sulfuric acid (H_2SO_4; PAni·H_2SO_4). The role of the secondary dopant is to diminish the polarization and to remove possible structural defects by the creation of a strong interaction with the PAni backbones and/or the primary dopant.[10,11] The main advantage of using a

Correspondence to: F. G. Souza, Jr (fgsj74@gmail.com).
Contract grant sponsor: Conselho Nacional de Desenvolvimento Científico e Tecnológico; contract grant numbers: 151616/2006-0, 577237/2008-0, 574358/2008-0, 307794/2008-3, 472009/2008-7.
Contract grant sponsor: Fundação Carlos Chagas Filho de Amparo à Pesquisa do Estado do Rio de Janeiro; contract grant number: E-26/112.116/2008.
Contract grant sponsor: Brazilian Synchrotron Light Laboratory.

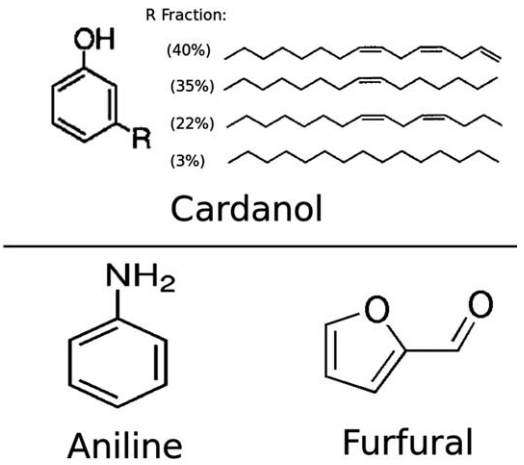

Figure 1 Used monomers.

secondary doping agent is that as demonstrated in previous studies,[12–14] the conductivity of PAni can be increased because of the development of more ordered structures and, consequently, enhanced charge mobility.

To increase the green characteristics of conducting polymer materials, polymer resins were prepared from mixtures of cardanol and furfural in the presence of H_2SO_4. Furfural is a product of the acid-catalyzed hydrolysis of polymeric pentoses (which can be obtained from corn cobs, oat and rice hulls, sugar-cane bagasse, and wood chips, among many other sources), followed by the acid-catalyzed dehydration of aldopentoses.[1,15] These resins were used here as biomatrices for the preparation of soft thermosetting conductive composites after *in situ* blending with PAni·H_2SO_4. Acid catalysis was selected to promote cardanol–furfural polymerizations because PAni·H_2SO_4 was used as the conductive filler. This was very important to prevent the dedoping of PAni·H_2SO_4. The obtained materials were characterized through X-ray scattering, Fourier transform infrared (FTIR) spectroscopy, and electrical conductivity and pressure sensitivity measurements. Pressure sensitivity and electromechanical analyses[16] indicated that the produced blends could be used as pressure-sensing materials. X-ray scattering experiments were also performed under pressure, as described in the literature, to allow for the improved interpretation of the pressure-sensitivity phenomenon.

EXPERIMENTAL

Materials

Aniline (analytical grade, Vetec, Rio de Janeiro, Brazil), ammonium peroxydisulfate (analytical grade, Vetec, Rio de Janeiro, Brazil), H_2SO_4 (analytical grade, Vetec, Rio de Janeiro, Brazil), furfural (analytical grade, Vetec, Rio de Janeiro, Brazil), and cardanol (kindly supplied by RESIBRAS Ltd., Fortaleza, Brazil) were used as received without any further purification.

Preparation of PAni·H_2SO_4

PAni was synthesized by the dispersion polymerization of aniline, as described in the literature.[17] In a typical procedure, 0.1 mol of aniline and 0.1 mol of H_2SO_4 were dissolved in 500 mL of distilled water and cooled in a refrigerating bath. Then, a solution containing 0.1 mol of ammonium peroxydisulfate and 80 mL of distilled water was added dropwise. The total polymerization time was 2 h. We terminated the polymerization by pouring the resulting polymer suspension into ethanol. The dark green PAni·H_2SO_4 powder was recovered, filtered, washed several times with ethanol, and dried *in vacuo* for 48 h at room temperature.

Resin preparation

The cardanol–furfural resin was prepared in accordance with the classical acid route[18] described for cardanol–formaldehyde reactions. In a typical procedure, cardanol and furfural were mixed together inside an Erlenmeyer flask under magnetic stirring. Afterward, a specified amount of H_2SO_4 was added to the mixture and kept under magnetic stirring for 3 min. The mass compositions of cardanol, furfural, and H_2SO_4 were always equal to 25 : 18 : 1. Resin samples were cast into small cylindrical polypropylene cups with dimensions of 30 mm diameter and 25 mm height. Because of the production of gaseous products during the polymerization, the preliminary mixing and polymerization were carried out in a fume-extraction chamber. The reactions were very exothermic and were performed at ambient temperature. Before complete conversion, different amounts of PAni were introduced into the polypropylene cups and mixed vigorously with the reacting bioresin.

Characterization

Infrared spectroscopy

FTIR experiments were performed in a PerkinElmer 1720X spectrometer with an wide band mercury cadmium telluride (MCT) and B– 400 cm^{-1} cutoff detector and a diffuse reflectance accessory (Waltham, MA).

X-ray scattering

High-resolution and high-intensity synchrotron X-ray diffraction (XRD) data were collected at the X-ray powder diffraction (XPD) beamline, placed after the D10B dipolar source of the Brazilian Synchrotron Light Laboratory (D10B-XPD 6651/07 and 7085/

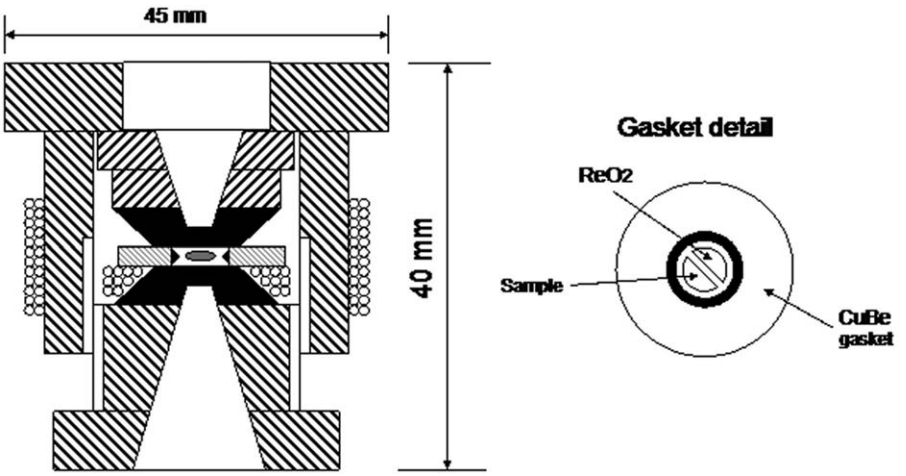

Figure 2 Schematic drawing of the B_4C anvil pressure cell with the following details: (a) the nonmagnetic CuBe cell body is shown by hash marks, (d) the B_4C anvil is black, and (c) the CuBe gasket is black. In both B_4C anvils, the largest diameter was 8×10^{-3} mm, and the smallest diameter was 4×10^{-3} mm. The gasket setup to XRD used the rhenium oxide (ReO_2) as an inner pressure gauge.

07).[19] X-rays of wavelength 1.24252(3) Å were selected by a double-bounce Si(111) monochromator with water refrigeration in the first crystal, whereas the second one was bent for sagittal focusing (Campinas, Brazil).[20] The beam was vertically focused or collimated by a bent Rh-coated ultra-low-expansion glass mirror placed before the monochromator, which also provided the filtering of high-energy photons (third-order and higher order harmonics). A vertically focused beam was used in the experiments, which delivered a flux of about 6×10^{10} photons/s at 100 mA and 10.535 keV in a spot of approximate dimensions of 1×10^{-3} m (vertical)$\times$ 2×10^{-3} m (horizontal) at the sample position. The experiments were performed in the vertical scattering plane, that is, perpendicular to the linear polarization of the incident photons. The wavelength and the zero point were determined from several well-defined reflections of the NIST SRM640c silicon standard. The diffracted beam was detected with a Na(Tl)I scintillation counter with a pulse-height discriminator in the counting chain. The incoming beam was also monitored by a scintillation counter for normalization of the decay of the primary beam. In this parallel-beam configuration, the resolution was determined by the slits in front of the detector. The samples were loaded into the copper berillyde (CuBe) pressure cell (see Fig. 2), which was kept at an incident θ angle of 8°, and data were recorded at room temperature for 40 s at each step of 0.007° from 5 to 30° [Bragg diffraction peak (2θ)].

Volume conductivity

Electrical conductivity measurements were performed with the conventional two-electrode method on pressed pellets of composite particles prepared at room temperature. Measurements were performed with a homemade sample holder coupled in a Tenma 72-6900 multimeter (Alpharetta, Georgia). The average diameter of the sample holder was 0.135 ± 0.03 mm, as described previously.[16,21–23]

Compression sensitivity

Samples were placed inside the sample holder. Soon afterward, the device containing the sample was positioned between the plates of a press (Carver 4350, Wabash, Indiana). Then, the samples were submitted to pressures of 0.0, 7.7, 15.5, 23.2, and 31.0 MPa. Simultaneously, the electrical resistivity test was performed with the Tenma 72-6900 multimeter. Data treatment was performed as presented previously.[16] In this case, the method can be summarized as follows:

1. The initial resistivity (R_0) was assumed to be equal to the resistivity (R) value obtained when $F = 0.4$ N [$P \approx 6300$ Pa], where F is the force and P is the pressure.
2. The percentage variation of the sample conductivity ($\Delta\sigma$) was calculated in accordance with eq. (1):

$$\Delta\sigma = \frac{100\left(R^{-1} - R_0^{-1}\right)}{R_0^{-1}} \quad (1)$$

3. The compression sensitivity (S_{comp}; %) was defined as

$$S_{c_{omp}} = \frac{\Delta\sigma}{\Delta P} \quad (2)$$

where ΔP is the variation of the applied pressure. Therefore, the dimensions of sensitivity to compression were expressed as percentage by megapascal.

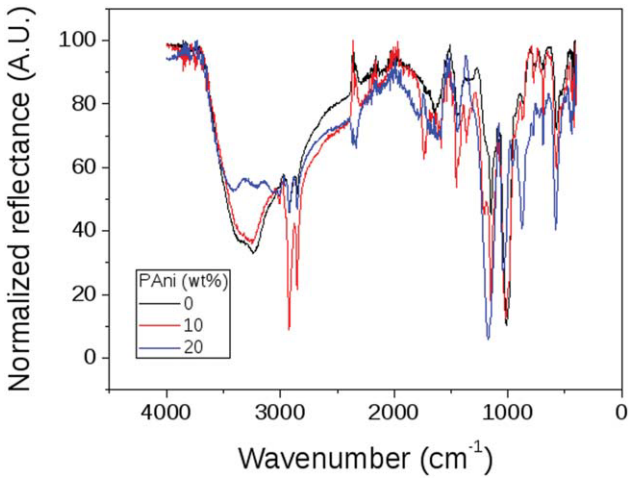

Figure 3 FTIR spectra of the bioresin and blended materials containing 10 and 20 wt % PAni. [Color figure can be viewed in the online issue, which is available at wileyonlinelibrary.com.]

RESULTS AND DISCUSSION

FTIR spectra of the cardanol and furfural bioresin (CFBR), and the CFBR blends with PAni (10 and 20 wt % PAni) are shown in Figure 3. The spectra of the CFBR samples were similar to that of a typical phenol–formaldehyde resin spectra. This spectrum in Figure 3 indicates that polymerization reactions occurred in the aromatic ring and that the unsaturated aliphatic chains were preserved. The wide band placed at 3250 cm^{-1} was related to the stretching of OH. This band was wide because the OH groups could form hydrogen bonds. The small characteristic band placed at 3000 cm^{-1} corresponded to the stretching of C—H, and the doublet at 2920 and 2850 cm^{-1} was related to the stretching of CH_2 and CH_3. The characteristic band at 1639 cm^{-1} was related to aliphatic C=C stretching. The band at 1438 cm^{-1} was characteristic of the C=C stretching of the aromatic ring. The bands at 1147 and 1012 cm^{-1} corresponded to the stretching of the C—O bond of the phenol group and the stretching of the C—O—C bond, respectively. Moreover, the characteristic band of the asymmetric stretching of the C=C bond in aromatic rings appeared around 960 cm^{-1}. Out-of-plane scissor deformation of adjacent hydrogen atoms of the aromatic ring appeared between 873 and 692 cm^{-1}. The band placed at 760 cm^{-1} was also characteristic of the asymmetric stretching of aliphatic CH_2. The band at 570 cm^{-1} was related to the stretching of the O—H bond.

When we compared the spectra of the pure cardanol–furfural bioresin with the ones of the blended materials, we observed some band displacements. The two characteristic bands located at 1735 and 1363 cm^{-1} seemed to be related to residual furfural. The first one was correlated to the C=O bond, which appeared conjugated with C=C of the aromatic ring. The last one was related to the scissoring deformation of the C—H bond of aldehyde. Spectra of the blends containing 10 and 20 wt % PAni showed no significant difference; this indicated that blending did not seem to affect the chemical nature of the final material.

Wide-angle X-ray scattering (WAXS) data for the biomatrix and its blends with PAni·H_2SO_4 are shown in Figure 4. This figure makes clear that the *in situ* blending process was able to produce a well-mixed material, which presented few crystalline peaks. In other words, the original PAni·H_2SO_4 structure was completely destroyed during the *in situ* blending with the bioresin and produced a homogeneously dispersed conducting material inside the biomatrix. This was certainly related to the chemical nature of the blended materials, as both species presented strong aromatic characteristics.[1] Despite that, as shown previously by the FTIR analyses, the chemical character of PAni·H_2SO_4 remained essentially the same.

WAXS data also provided information about the degree of crystallinity[24–37] and the doping state[23,38–40] of the PAni domains. This is very important because highly ordered materials can lead to higher electrical conductivities.[23,38–42] According to Pouget et al.,[43] PAni possesses a pseudo-orthorhombic unit cell structure, characterized by 2θ's of 20.2, 21.6, 26.7, 29.8, and 34.6°. WAXS of the pure PAni·H_2SO_4 and respective 2θ's are shown in Table I. In Table I, the interplanar distance (*d*) was calculated in accordance with Bragg's law, whereas the crystal size (CS) was obtained with the help of Scherrer's equation [eq. (3)]:

$$CS = K\lambda/\Delta \times cos\theta \tag{3}$$

where *K* is a constant (equal to 1.0 here), λ is the wavelength, θ is the Bragg angle (=2θ/2), and Δθ

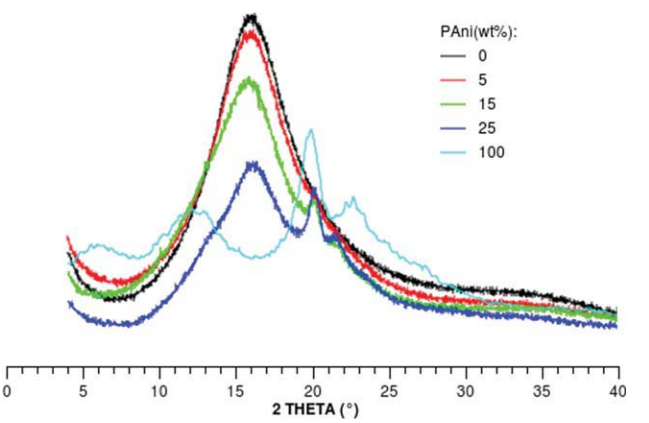

Figure 4 WAXS patterns of the CFBR, blended materials, and pure PAni. [Color figure can be viewed in the online issue, which is available at wileyonlinelibrary.com.]

TABLE I
WAXS Peaks of Pure PAni·H_2SO_4

Peak	Center (°)	Height	Area	fwhm (°)	CS (Å)[a]	d (Å)[b]
1	6.328	0.10	0.31	3.01	0.41	11.26
2	12.070	0.27	1.19	4.15	0.30	5.91
3	19.809	0.42	0.64	1.44	0.88	3.61
4	22.085	0.28	3.09	10.29	0.12	3.24
5	22.622	0.12	0.21	1.64	0.77	3.17
6	27.364	0.02	0.02	0.73	1.75	2.63

[a] From Scherrer's equation.
[b] From Bragg's law.

is the full width at half-maximum (fwhm) of the peak.

Among the peaks presented in Table I, the ones centered at 19.8° ($d \approx 3.6$ Å) and 24.7° ($d \approx 2.6$ Å) were regarded as the most important. The peak centered around 20° (100 face) represented the characteristic distance between the ring planes of benzene rings in adjacent chains (or the close-contact interchain distance), whereas the peaks around 25° (110 face) may have been due to oscillations along the plane that was orthogonal to the polymer chain.[40,43–46] In this case, the peak at 25° was weaker than the one at 20° (100-face); this indicated that a highly doped state was not reached.[40,43]

The previous results were supported by the small crystallinity degree of pure PAni, which was equal to 48 ± 4% in this case and could be regarded as small compared to the 80% of crystallinity reported by Gospodinova et al.[47] Despite that, samples of pure PAni presented an electrical conductivity of (2.8 ± 0.2) × 10^{-1} S/cm. This conductivity value indicated that the prepared PAni samples presented semiconductor behavior and could be used in pressure-sensitive devices.[16,22,23]

Table II presents the volume conductivity of the bioresin/PAni blends as a function of the PAni content. The percolation threshold was calculated in accordance with a very simple model,[22] as shown in eq. (4):

$$\mathrm{Log}V_c = A + B \times \mathrm{Log}(\mathrm{PAni–PT}) \quad (4)$$

where V_c is the volume conductivity, PAni is the PAni·H_2SO_4 concentration (wt %), PT is the percolation threshold, and A and B are model parameters

TABLE II
Volume Conductivity of the Studied Materials

PAni (wt %)	V_c (S/cm)
0	(1.77 ± 0.09) × 10^{-8}
5	(2.9 ± 0.1) × 10^{-8}
10	(9.1 ± 0.5) × 10^{-8}
15	(3.5 ± 0.2) × 10^{-6}
20	(1.68 ± 0.08) × 10^{-3}
25	(8.7 ± 0.4) × 10^{-3}
100	(2.78 ± 0.02) × 10^{-1}

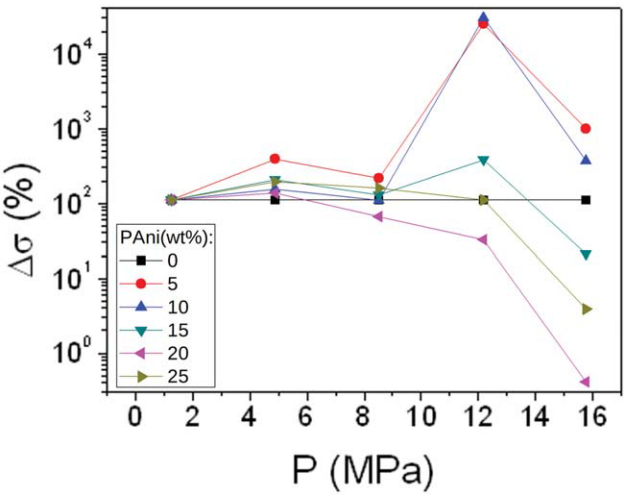

Figure 5 Conductivity variation as a function of the applied pressure. [Color figure can be viewed in the online issue, which is available at wileyonlinelibrary.com.]

equal to 4.9 ± 0.2 wt % (−20.52 ± 0.09 and 13.28 ± 0.07, respectively). The percolation model led to a very good correlation, equal to 0.982. A significant decrease in the resistivity was obtained after blending, and the maximum reduction of the resistivity was attained when the PAni·H_2SO_4 content reached 9 wt % (the resistivity was 3 × 10^4 times lower in this blend). These blends could also be regarded as semiconductors and could be used as compression-sensitive materials.[14,16]

The compression sensitivities of the tested materials are shown in Figure 5. All samples presented a slight increase in electrical conductivity with pressure until the 7.7-MPa limit. The blend containing 5 wt % PAni presented the larger variation of conductivity (~ 340%). The increase of the PAni concentration led to a decrease in the conductivity variation, which could be related to the increasing number of contact points among the PAni chains.

Above 7.7 MPa, a very interesting behavior was noticed. This behavior seemed to be connected with the percolation limit, as samples containing amounts of PAni below the percolation threshold showed the biggest conductivity variations. This behavior was intimately related to the increase in the number of contact points among PAni chains, as described previously. Samples containing 5 and 10 wt % PAni presented conductivity variations of 18,100 and 21,700% at 11.6 MPa. Further increases in the compressive pressure led to a decrease in the conductivity variation. This was probably due to the Poisson effect, which caused the separation of the electrical contact points of the blend.[16,17] Samples containing 15, 20, and 25 wt % PAni presented higher conductivity values but lower conductivity variations, as the large number of electric contact points could not be significantly increased through pressure

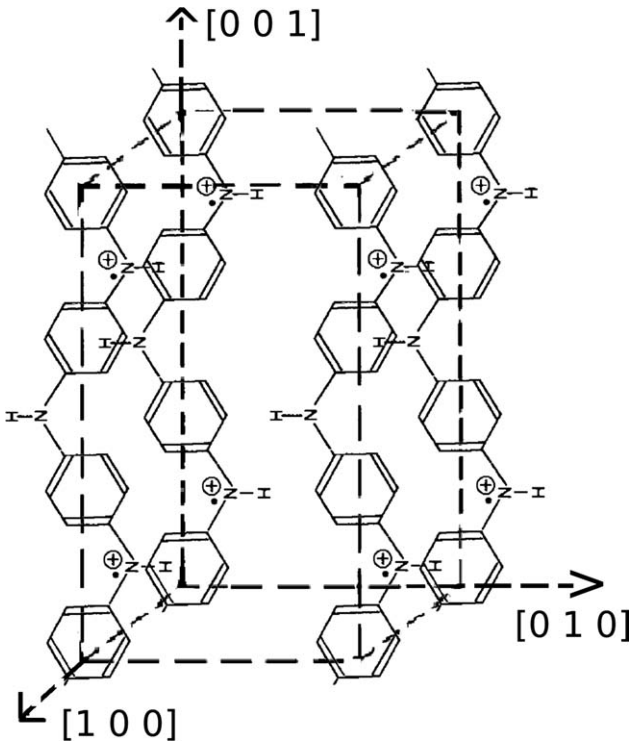

Figure 6 Orthorhombic primitive unit cell of the PAni.

variations. So, among the tested materials, the most promising ones were those prepared with 10 wt % PAni or less. Blends containing 5 wt % PAni can be recommended because of the higher pressure sensitivity of electrical conductivity and smaller PAni concentration, which would be useful both from economic and environmental points of view. It is important to say that despite the relatively low electrical conductivity, these blends could be useful for the manufacturing of pressure-sensitive devices, as discussed in the literature.[22]

The model proposed by Luzny et al.[48] indicated that DPHP-protonated PANI formed an orthorhombic primitive unit cell, with the lattice constants *a* (100), *d* (010), and *c* (001) fitted as 4.4, 5.6, and 7.2 Å, respectively, which were associated with an orthorhombic cell,[49] as shown in Figure 6. Figure 7 shows the XRD experimental data obtained under pressure. Gaussian deconvolution was also present, on the basis of the crystalline model proposed by Luzny et al.[48]

As shown in Figure 4, diffraction signals were only detectable when the PAni composition was equal to or larger than 15 wt %. According to Giles et al.[19] and Ferreira et al.,[20] the boron carbide (B_4C) anvil in the high-pressure cell used here showed good transparency when the measurements were performed at 10.535 keV. The normalized diffraction peaks of the B_4C anvil ($\sim 28.1^\circ$ 2θ) were right-shifted because of the unit cell compression, which was used as an inner pressure gauge. The diffraction peaks of the B_4C anvil needed to be carefully subtracted from the diffraction patterns for each pressure measurement to unveil the real effect of the hydrostatic pressure[19,20] on the PAni. After subtraction, the signal-to-noise ratio was maximized for the sample containing 25 wt % PAni, whereas the signal-to-noise ratio was very low for the sample containing 5 wt % PAni. This effect was due to the high scattering factor provided by high amounts of PAni. For this reason, to improve the quantitative analysis of the external pressure effect on the PAni crystallographic symmetry (increase of signal-to-noise relation), the sample containing 25 wt % PAni was selected for a more detailed analytical study. Despite the higher amounts of PAni, as the scale of the scattering phenomena was in the range of 30 pm and all blends were exposed to the same hydrostatic pressure, it was assumed here that results obtained with 25 wt % PAni were able to represent those of all of the other blends.

Table III shows the shift of crystalline peaks and respective *d* values under pressure for the sample containing 25 wt % PAni. The crystalline distance between (010) planes showed no changes with pressure increments, possibly because of the compact assembly of the intermolecular rings that occupied the same unit cell face. The distance of about 5.3 Å between adjacent (010) faces was very similar to the size of these rings, 5–6 Å. The data shown in Table III indicate that the distance between adjacent (001) planes increased and that the distance between (100) planes decreased when samples containing 25 wt % PAni were exposed to pressure increments. The decrease in the crystalline distance between (100) planes with pressure increment were related to the increase of the crystalline distance between (001)

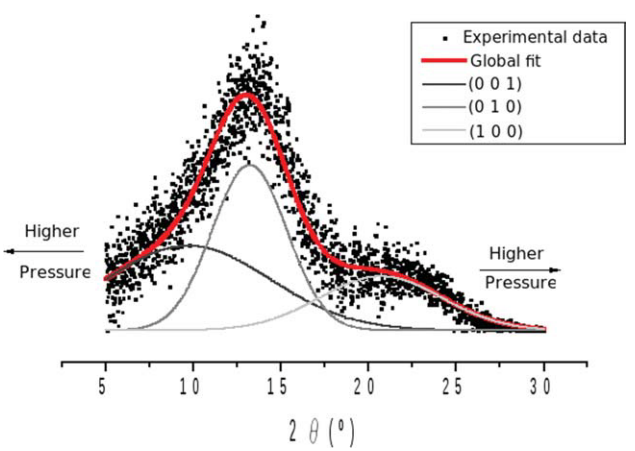

Figure 7 XRD experimental data under pressure and Gaussian deconvolution. [Color figure can be viewed in the online issue, which is available at wileyonlinelibrary.com.]

TABLE III
Blend Containing 25 wt % of PAni: Shift of the Crystalline Peaks and Respective *d* Values Under Pressure

Pressure (MPa)			
Peak center (°)			
	(001)	(010)	(100)
2.5	9.96 ± 0.09	13.2 ± 0.1	20.68 ± 0.06
5	9.68 ± 0.08	13.8 ± 0.2	21.78 ± 0.06
7.5	9.51 ± 0.06	13.4 ± 0.1	21.97 ± 0.03
Crystalline distance (Å)			
	(001)	(010)	(100)
2.5	7.16 ± 0.04	5.4 ± 0.1	3.46 ± 0.01
5	7.36 ± 0.05	5.2 ± 0.1	3.29 ± 0.01
7.5	7.49 ± 0.04	5.3 ± 0.1	3.26 ± 0.01

planes, as both effects were probably caused by the reduction of entropy of the polymer chains.

Although electrical changes under compression were certainly related to larger scale phenomena that could be observed by small-angle X-ray scattering, these results indicate that PAni chains were considerably disturbed by compressive stresses. To the best of our knowledge, this type of characterization has not been performed previously for PAni samples, blends, or composites.

CONCLUSIONS

With the focus on environment issues, the obtained materials were very encouraging because they presented interesting electrical responses, even with low amounts of PAni. In addition, the FTIR results indicate that the insertion of the PAni in the blends did not change the chemical nature of the resin. They also may have indicated that chemical bound sites, able to promote the biodegradable characteristic of the pure resin, remained available.

Some of these properties were intimately related to the morphology of the blended materials, where the resin and PAni were, according WAXS results, intimately mixed together. This kind of morphology is important to compression sensitivity once a deeper dispersion of conducting particles can produce materials able to suffer the largest electrical conductivity changes under pressure. This conclusion was supported by the electromechanical tests, which showed that the obtained blends could be useful as pressure-sensitive materials. In addition, among the tested materials, blends containing around 5 wt % PAni·H_2SO_4 presented the largest compression-sensitivity values. This result must be highlighted because the blend containing 5 wt % PAni showed the highest variation of the electrical conductivity under pressure with the lowest amount of PAni in the blends; this may possibly provide a biodegradable sensing material. Finally, it was shown for the first time, through DRX analyses under pressure, that PAni chains were considerably disturbed by compressive stresses.

The authors thank the Brazilian Synchrotron Light Laboratory for technical and financial support with the DRX and WAXS/small-angle X-ray scattering experiments.

References

1. Souza, F. G. Jr.; Richa, P.; Siervo, A.; Oliveira, G. E.; Rodrigues, C. H. M.; Nele, M.; Pinto; J. C. Macromol Mater Eng 2008, 293, 675.
2. Souza, F. G Jr.; Pinto, J. C.; Rodrigues, M. V.; Anzai, T. K.; Richa, P.; Melo, P. A.; Nele, M.; Oliveira, G. E.; Soares, B. G. Polym Eng Sci 2008, 48, 1947.
3. Griffith, L. G. Acta Mater 2000, 48, 263.
4. Gruber, P. R. Carbon Management: Implications for R & D in the Chemical Sciences and Technology; National Academic: Washington, DC, 2001; p 166.
5. Gross, R. A.; Kalra, B. Science 2002, 297, 803.
6. Slater, S.; Glassner, D.; Vink, E.; Gerngross, T. In Biopolymers; Wiley: New York, 2006; p XVI/474.
7. Miyata, S.; Techagumpuch, A. Synth Met 1989, 31, 311.
8. Sun, Y.; MacDiarmid, A. G.; Epstein, A. J. J Chem Soc Chem Commun 1990, 7, 529.
9. Toyomizu, M.; Okamoto, K.; Ishibashi, T.; Chen, Z.; Nakatsu, T. Life Sci 1999, 66, 229.
10. Ikkala, L.-O.; Pietila, L.; Ahjopalo, H.; Osterholm, H.; Passiniemi, P. J. J Chem Phys 1995, 103, 9855.
11. Vikki, T.; Pietila, L. O.; Osterholm, H.; Ahjopalo, L.; Taka, A.; Toivo, A.; Levon, K.; Passiniemi, P.; Ikkla, O. Macromolecules 1996, 29, 2945.
12. Souza, F. G. Jr.; Soares, B. G.; Siddaramaiah. Polymer 2006, 47, 2163.
13. Souza, F. G. Jr.; Soares, B. G.; Pinto, J. C. Eur Polym J 2007, 43, 2007.
14. Souza, F. G. Jr.; Pinto, J. C.; Oliveira, G. E.; Soares, B. G.. Polym Test 2007, 26, 720.
15. Martínez-García, A.; Ortiz, M.; Martínez, R; Ortiz, P.; Reguera, E. Ind Crops Prod 2004, 19, 99.
16. Souza, F. G. Jr.; Michel, R. C.; Soares, B. G.. Polym Test 2005, 24, 998.
17. Souza, F. G. Jr.; Anzai, T. K.; Melo, P. A.; Soares, B. G.; Nele, M.; Pinto, J. C. J Appl Polym Sci 2008, 107, 2404.
18. Bisanda, E. T. N.; Ansell, M. P.. J Mater Sci 1992, 27, 1690.
19. Giles, C.; Yokaichiya, F.; Kycia, S. W.; Sampaio, L. C.; Ardiles-Saraiva, D. C.; Franco, M. K. K.; Neuenschwander, R. T. J Synchrotron Radiat 2003, 10, 430.
20. Ferreira, F. F.; Corrêa, H. P. S.; Orlando, M. T. D.; Passamai, J. L. Jr.; Orlando, C. G. P.; Cavalcante, I. P.; Garcia, F.; Tamura, E.; Martinez, L. G.; Rossi, J. L.; Melo, F. C. L. J Synchrotron Radiat 2009, 16, 48.
21. Souza, F. G. Jr.; Soares, B. G.; Dahmouche, K. J Polym Sci Part B: Polym Phys 2007, 45, 3069.
22. Souza, F. G. Jr.; Almeida, M.; Soares, B. G.; Pinto, J. C. Polym Test 2007, 26, 692.
23. Souza, F. G. Jr.; Soares, B. G.; Pinto, J. C. Eur Polym J 2008, 44, 3908.
24. Kim, T. H.; Lim, S. T.; Lee, C. H.; Choi, H. J.; Jhon, M. S. J Appl Polym Sci 2003, 87, 2106.

25. Wan, M. X.; Li, M.; Li, J. C.; Liu, Z. X. J Appl Polym Sci 1994, 53, 131.
26. Shinde, V.; Sainkar, S. R.; Patil, P. P. J Appl Polym Sci 2005, 96, 685.
27. Chaudhari, H. K.; Kelkar, D. S. J Appl Polym Sci 1996, 62, 15.
28. Souza, F. G., Jr.; Sirelli, L.; Michel, R. C.; Soares, B. G.; Herbst, M. H. J Appl Polym Sci 2006, 102, 535.
29. Yu, Y. H.; Jen, C. C.; Huang, H. Y.; Wu, P. C.; Huang, C. C.; Yeh, J. M. J Appl Polym Sci 2004, 91, 3438.
30. Athawale, A. A.; Bhagwat, S. V. J Appl Polym Sci 2003, 89, 2412.
31. Yeh, J. M.; Chin, C. P.; Chang, S. J Appl Polym Sci 2003, 88, 3264.
32. Naidu, B. V. K.; Bhat, S. D.; Sairam, M.; Wali, A. C.; Sawant, D. P.; Halligudi, S. B.; Mallikarjuna, N. N.; Aminabhavi, T. M. J Appl Polym Sci 2005, 96, 1968.
33. Yu, Y. H.; Yeh, J. M.; Liou, S. J.; Chen, C. L.; Liaw, D. J.; Lu, H. Y. J Appl Polym Sci 2004, 92, 3573.
34. Kim, J. W.; Jang, L. W.; Choi, H. J.; Jhon, M. S. J Appl Polym Sci 2003, 89, 821.
35. Yeh, J. M.; Chin, C. P. J Appl Polym Sci 2003, 88, 1072.
36. Han, M. G.; Im, S. S. J Appl Polym Sci 1999, 71, 2169.
37. Chen, C. H. J Appl Polym Sci 2003, 89, 2142.
38. Han, M. G.; Cho, S. K.; Oh, S. G.; Im, S. S. Synth Met 2002, 126, 53.
39. Li, Z. F.; Kang, E. T.; Neoh, K. G.; Tan, K. L. Synth Met 1997, 87, 45.
40. Li, Z. F.; Neoh, K. G.; Pun, M. Y.; Kang, E. T.; Tan, K. L. Synth Met 1995, 73, 209.
41. Abdiryim, T.; Xiao-Gang, Z.; Jamal, R. Mater Chem Phys 2005, 90, 367.
42. Souza, F. G. Jr.; Soares, B. G.; Siddaramaiah. Polymer 2006, 47, 2163.
43. Pouget, J. P.; Jozefowicz, M. E.; Epstein, A. J.; Tang, X.; MacDiarmid, A. G. Macromolecules 1991, 24, 779.
44. Moon, Y. B.; Cao, Y.; Smith, P.; Heeger, A. J.. Polym Commun 1989, 30, 196.
45. Pouget, J. P.; Hsu, C. H.; MacDiarmid, A. G.; Epstein, A. J. Synth Met 1995, 69, 119.
46. Souza, F. G. Jr.; Soares, B. G.; Siddaramaiah, P. J Phys 2007, 69, 435.
47. Gospodinova, N.; Ivanov, D. A.; Anokhin, D. V.; Mihai, I.; Vidal, L.; Brun, S.; Romanova, J.; Tadjer, A. Macromol Rapid Commun 2008, 30, 29.
48. Luzny, W.; Kaniowski, T.; Pron, A. Polymer 1998, 39, 475.
49. Djurado, D.; Nicolau, Y. F.; Dalsegg, L.; Samuelsen, E. J. Synth Met 1997, 84, 121.